# Chemistry of the Phenoxathiins and Isosterically Related Heterocycles. XXVII. Two-Dimensional J-Resolved Spectra of 1,4,9-Triazaphenoxathiin: The Influence of Frequency of the Position and Intensity of Resonances Due to Strong Coupling [1]

Gary E. Martin [2] and Robert T. Gampe, Jr.

Department of Medicinal Chemistry, College of Pharmacy, University of Houston, Houston, Texas 77004, U.S.A.

Joseph J. Ford and M. Robert Willcott, III

Department of Chemistry, University of Houston, Houston, Texas 77004, U.S.A.

Michael Morgan and Andrew L. Ternay, Jr.

Department of Chemistry, University of Texas at Arlington, Arlington, Texas 76019, U.S.A.

Charles O. Okafor [3]

Department of Chemistry, Faculty of Physical Sciences, University of Nigeria, Nsukka, Nigeria

Keith Smith

Department of Chemistry, University College of Swansea, Singleton Park, Swansea SA2 8PP, U.K.

Received December 9, 1982

The synthesis of 1,4,9-triazaphenoxathiin and the analysis of the two-dimensional J-resolved (2DJ) $^1$H-nmr spectra of the molecule at 100 and 200 MHz are reported. Due to the strong coupling of the ABX and AB spin systems, additional resonances are observed in the 100 MHz 2DJ spectrum which are diminished in intensity and shifted further from $F^1 = 0$ Hz in the case of the ABX system at 200 MHz, or which have disappeared in the 200 MHz spectrum in the case of the AB spin system. Calculated frequencies and intensities of the resonances due to strong coupling were found to be in excellent agreement with the observed data.

*J. Heterocyclic Chem.*, **20**, 1063 (1983).

Conceptually, two-dimensional Fourier transform nmr (2DFT nmr) is now ten years old [4]. Experimental 2DFT nmr was implemented in 1975, four years after the suggestion of the experiment. In the first report of an experimental spectrum, Muller, Kumar and Ernst [5] demonstrated the general heteronuclear cross-correlated 2DFT nmr experiment, their methodology differing from that proposed by Jeener [4] in several important respects. The Jeener pulse sequence, associated with auto-correlated two-dimensional nmr, was subsequently executed [6], and is the basis for several useful experiments [7]. Two dimensional J-resolved (2DJ) homonuclear spectroscopy was first reported in 1976 [8]. That report, highlighting the exciting new vistas accessable by these techniques, was followed by numerous other papers which have dealt with various aspects of the two-dimensional experiment which include but are by no means limited to: calculation and analysis of 2DJ spectra [9-11]; projections of data contained in two-dimensional spectra [12,13]; tilting of phase modulated two-dimensional spectra to facilitate spin-multiplet extraction [14]; and studies of the effects of strong coupling in 2DJ spectra [15-17]. We wish to report the synthesis of 1,4,9-triazaphenoxathiin (**6**) and its use as an nmr model compound. The analysis of the 2DJ $^1$H-nmr spectra of the molecule at 100 and 200 MHz illustrates the effects of spectrometer operating frequency in the minimization of resonances due to strong coupling.

The synthesis of the 1,4,9-triazaphenoxathiin (**6**) utilized in this study employed the condensation of 2,3-dichloropyrazine (**2**), prepared according to the method of Okafor [18], with the disodium salt of 3-hydroxypyridine-2(1*H*)-thione (**3**) in *N,N*-dimethylformamide as shown in Scheme I.

**SCHEME I**

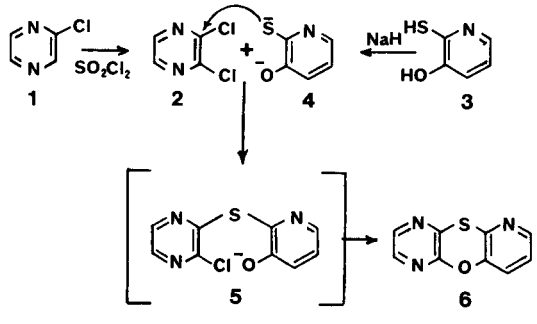

Although no effort was made to isolate the intermediate phenolate-sulfide, it is presumed that this reaction proceeded without a Smiles rearrangement unlike the recently reported reaction of 4,5-dichloro-6(1*H*)-pyridazinone with the disodium salt of *o*-mercaptophenol which does undergo rearrangement in addition to direct cyclization [19].

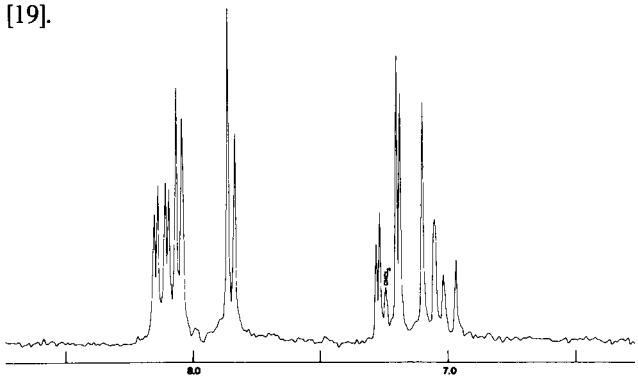


Figure 1. $^1$H-nmr spectrum of 1,4,9-triazaphenoxathiin (**6**) in deuteriochloroform at 100 MHz (note the pseudo-first order character of the ABX spin system resonances).

Examination of the proton nmr spectrum of **6** taken in the conventional manner (Figure 1) at 100 MHz showed five well resolved, pseudo-first order multiplets arising from the ABX and AB spin systems in the pyridine and pyrazine portions of the molecule respectively. The proton spectrum of **6** at 200 MHz, in contrast, was nearly first order for the ABX portion of the spectrum. It is this difference between the two spectra which makes the compound ideally suited as a model system with which to illustrate and understand the frequency dependent features of 2DJ spectra, and to produce model data useful in the eventual study of more complex systems.

Acquisition of the Two-Dimensional NMR-Spectra.

Two-dimensional J-resolved homonuclear nmr spectra of **6** were taken on spectrometers operating at frequencies of 100 and 200 MHz for protons observation. The initial $S(t_1, t_2)$ data sets were obtained using 1K and 2K data points in $t_2$ at 100 and 200 MHz respectively, with 256 values of $t_1$ employed in both experiments to give comparable digitization in both final two-dimensional nmr

Table I

Frequencies and Intensities of the AB Transitions in the 2DJ Spectrum of an ABX Spin System

| Line pqrs | $F_1$ | $F_2$ (a) | I |
|---|---|---|---|
| 1368 | $\frac{1}{2}(D_+ - D_- - J_{AB} - \frac{1}{2}J_{AX} - \frac{1}{2}J_{BX})$ | $-D_- - \frac{1}{2}J_{AB} - \frac{1}{4}J_{AX} - \frac{1}{4}J_{BX}$ | $\cos\Sigma(\cos\Sigma + \sin\Delta)$ |
| 2547 | $\frac{1}{2}(D_- - D_+ - J_{AB} + \frac{1}{2}J_{AX} + \frac{1}{2}J_{BX})$ | $-D_+ - \frac{1}{2}J_{AB} + \frac{1}{4}J_{AX} + \frac{1}{4}J_{BX}$ | $\cos\Sigma(\cos\Sigma - \sin\Delta)$ |
| 1458 | $\frac{1}{2}(D_- - D_+ - J_{AB} - \frac{1}{2}J_{AX} - \frac{1}{2}J_{BX})$ | $+D_- - \frac{1}{2}J_{AB} - \frac{1}{4}J_{AX} - \frac{1}{4}J_{BX}$ | $\cos\Sigma(\cos\Sigma - \sin\Delta)$ |
| 2637 | $\frac{1}{2}(D_+ - D_- - J_{AB} + \frac{1}{2}J_{AX} + \frac{1}{2}J_{BX})$ | $+D_+ - \frac{1}{2}J_{AB} + \frac{1}{4}J_{AX} + \frac{1}{4}J_{BX}$ | $\cos\Sigma(\cos\Sigma + \sin\Delta)$ |
| 1358 | $\frac{1}{2}(D_+ + D_- - J_{AB} - \frac{1}{2}J_{AX} - \frac{1}{2}J_{BX})$ | $+D_- - \frac{1}{2}J_{AB} - \frac{1}{4}J_{AX} - \frac{1}{4}J_{BX}$ | $\sin\Sigma(\cos\Sigma + \sin\Delta)$ |
| 2537 | $\frac{1}{2}(D_+ + D_- - J_{AB} + \frac{1}{2}J_{AX} + \frac{1}{2}J_{BX})$ | $+D_+ - \frac{1}{2}J_{AB} + \frac{1}{4}J_{AX} + \frac{1}{4}J_{BX}$ | $\sin\Sigma(\cos\Sigma + \sin\Delta)$ |
| 2647 | $-\frac{1}{2}(D_+ + D_- + J_{AB} - \frac{1}{2}J_{AX} - \frac{1}{2}J_{BX})$ | $-D_+ - \frac{1}{2}J_{AB} + \frac{1}{4}J_{AX} + \frac{1}{4}J_{BX}$ | $\sin\Sigma(\cos\Sigma - \sin\Delta)$ |
| 1468 | $-\frac{1}{2}(D_+ + D_- + J_{AB} + \frac{1}{2}J_{AX} + \frac{1}{2}J_{BX})$ | $-D_- - \frac{1}{2}J_{AB} - \frac{1}{4}J_{AX} - \frac{1}{4}J_{BX}$ | $\sin\Sigma(\cos\Sigma - \sin\Delta)$ |
| 6813 | $-\frac{1}{2}(D_+ - D_- - J_{AB} - \frac{1}{2}J_{AX} - \frac{1}{2}J_{BX})$ | $-D_+ + \frac{1}{2}J_{AB} + \frac{1}{4}J_{AX} + \frac{1}{4}J_{BX}$ | $\cos\Sigma(\cos\Sigma + \sin\Delta)$ |
| 4725 | $-\frac{1}{2}(D_- - D_+ - J_{AB} + \frac{1}{2}J_{AX} + \frac{1}{2}J_{BX})$ | $-D_- + \frac{1}{2}J_{AB} - \frac{1}{4}J_{AX} - \frac{1}{4}J_{BX}$ | $\cos\Sigma(\cos\Sigma - \sin\Delta)$ |
| 5814 | $-\frac{1}{2}(D_- - D_+ - J_{AB} - \frac{1}{2}J_{AX} - \frac{1}{2}J_{BX})$ | $+D_+ + \frac{1}{2}J_{AB} + \frac{1}{4}J_{AX} + \frac{1}{4}J_{BX}$ | $\cos\Sigma(\cos\Sigma - \sin\Delta)$ |
| 3726 | $-\frac{1}{2}(D_+ - D_- - J_{AB} + \frac{1}{2}J_{AX} + \frac{1}{2}J_{BX})$ | $+D_- + \frac{1}{2}J_{AB} - \frac{1}{4}J_{AX} - \frac{1}{4}J_{BX}$ | $\cos\Sigma(\cos\Sigma + \sin\Delta)$ |
| 5813 | $-\frac{1}{2}(D_+ + D_- - J_{AB} - \frac{1}{2}J_{AX} - \frac{1}{2}J_{BX})$ | $-D_+ + \frac{1}{2}J_{AB} + \frac{1}{4}J_{AX} + \frac{1}{4}J_{BX}$ | $\sin\Sigma(\cos\Sigma + \sin\Delta)$ |
| 3725 | $-\frac{1}{2}(D_+ + D_- - J_{AB} + \frac{1}{2}J_{AX} + \frac{1}{2}J_{BX})$ | $-D_- + \frac{1}{2}J_{AB} - \frac{1}{4}J_{AX} - \frac{1}{4}J_{BX}$ | $\sin\Sigma(\cos\Sigma + \sin\Delta)$ |
| 4726 | $\frac{1}{2}(D_+ + D_- + J_{AB} - \frac{1}{2}J_{AX} - \frac{1}{2}J_{BX})$ | $+D_- + \frac{1}{2}J_{AB} - \frac{1}{4}J_{AX} - \frac{1}{4}J_{BX}$ | $\sin\Sigma(\cos\Sigma - \sin\Delta)$ |
| 6814 | $\frac{1}{2}(D_+ + D_- + J_{AB} + \frac{1}{2}J_{AX} + \frac{1}{2}J_{BX})$ | $+D_+ + \frac{1}{2}J_{AB} + \frac{1}{4}J_{AX} + \frac{1}{4}J_{BX}$ | $\sin\Sigma(\cos\Sigma - \sin\Delta)$ |

(a) from $\frac{\nu_A + \nu_B}{2}$

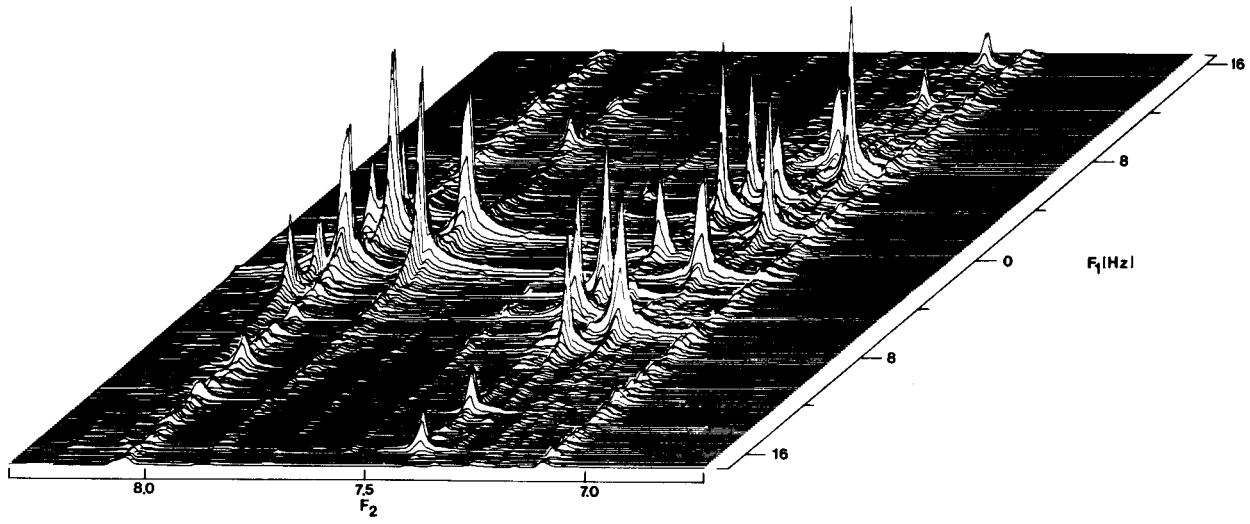


Figure 2A. White-washed stack plot of the $S(F_1,F_2)$ data matrix from the homonuclear 2DJ spectrum 1,4,9-triazaphenoxathiin (**6**) in deuteriochloroform at 100 MHz. (Only the region ± 16 Hz in $F_1$ was plotted - no peaks were observed outside of this region of the spectrum.)

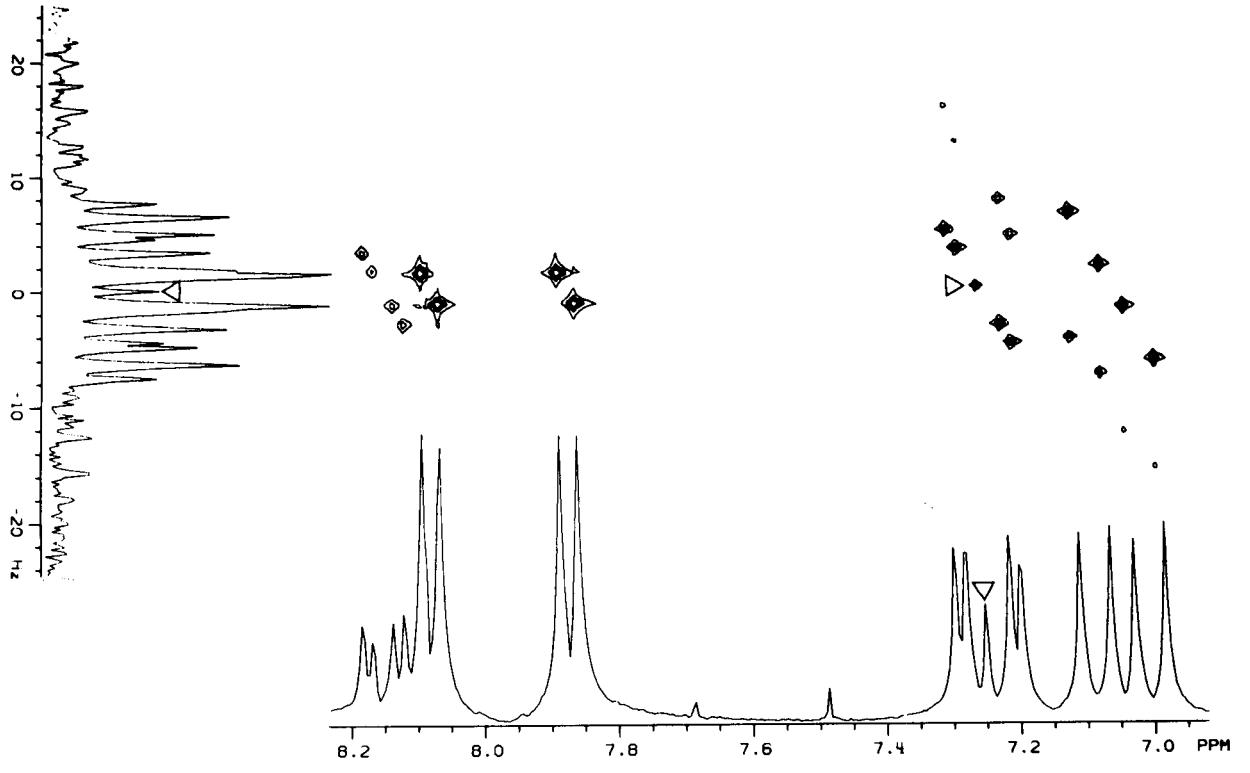


Figure 2B. Four level contour plot of the homonuclear 2DJ spectrum of 1,4,9-triazaphenoxathiin (**6**) in deuteriochloroform at 100 MHz. The spectrum was plotted from the $S(F_2,F_1)$ data matrix prior to tilting. The normal spectrum ($F_2$) was obtained from the 90° projection of the data matrix while the J-spectrum was obtained from a 0° projection. Responses designated with open triangles are due to residual protiochloroform.

spectra. Delay values employed in the incrementation of $t_1$ through the series of experiments performed were chosen to give a final spectral width of ± 25 Hz in $F_1$ upon completion of the data processing.

The 100 MHz 2DJ $^1$H-nmr spectrum of **6** is shown in Figure 2A as a white-washed stack plot and in Figure 2B as a four level coutour plot. Note that there are substantially more resonances in the upfield segment of the spec-

trum due to the A and B resonances of the ABX spin system than would be anticipated solely on the basis of first-order scalar coupling considerations. In addition to the anticipated doublet of doublets for A and B, there are eight additional resonances present which arise from strong coupling [15,17] and which further, are accounted for in the calculation of the 2DJ spectra [9-11] discussed below. The upfield region of the 200 MHz 2DJ $^1$H-nmr spectrum of **6** (Figure 3), in contrast, shows that these resonances are still present but with reduced intensity and with greater separation relative to 0 Hz on the $F_1$ axis as a result of the increased observation frequency.

Analysis of The J-Resolved Spectra as a Function of Spectrometer Frequency.

It is clearly redundant to advise any competent spectroscopist to utilize the highest field spectrometer available for a given investigation. Indeed, the analysis of spectra which are complicated by spin-multiplet overlap at one frequency is often simplified by resorting to a higher field spectrum. In a similar sence, 2DJ $^1$H-nmr spectra may be thought of as being analogous to the higher field spectrum in that spin-multiplet overlapping is circumvented since scalar (J) coupling information is displayed along $F_1$, orthogonal to the chemical shift information which appears along $F_2$. It might therefore appear a logical decision on the part of a novice user of two-dimensional nmr to resort to a 2DJ spectrum rather than going to a higher spectrometer. While this is a perfectly satisfactory solution in many cases, it is by no means the appropriate solution to all interpretation problems. In the case of molecules containing strongly coupled spin systems (for example the ABX and AB spin systems of **6**), the pseudo-first or higher order character of these spectra may lead to intense resonances in the 2DJ spectra in addition to the anticipated multiplet resonances [15,17], which may thus serve to complicate rather than to simplify the appearance of the spectrum. These features are conveniently illustrated in the 2DJ spectra of **6** at 100 and 200 MHz (Figures 2B and 3 respectively).

Individual spin-multiplets in J-resolved spectra are symmetric about $F_1 = 0$ Hz in the case where a non-selective 180° pulse is applied to the spin system [9,10]. This observation is in contrast to the conventional spectrum in which the same spin multiplet may completely lack symmetry. Although the symmetry of the 2DJ spectrum is cosmetical-

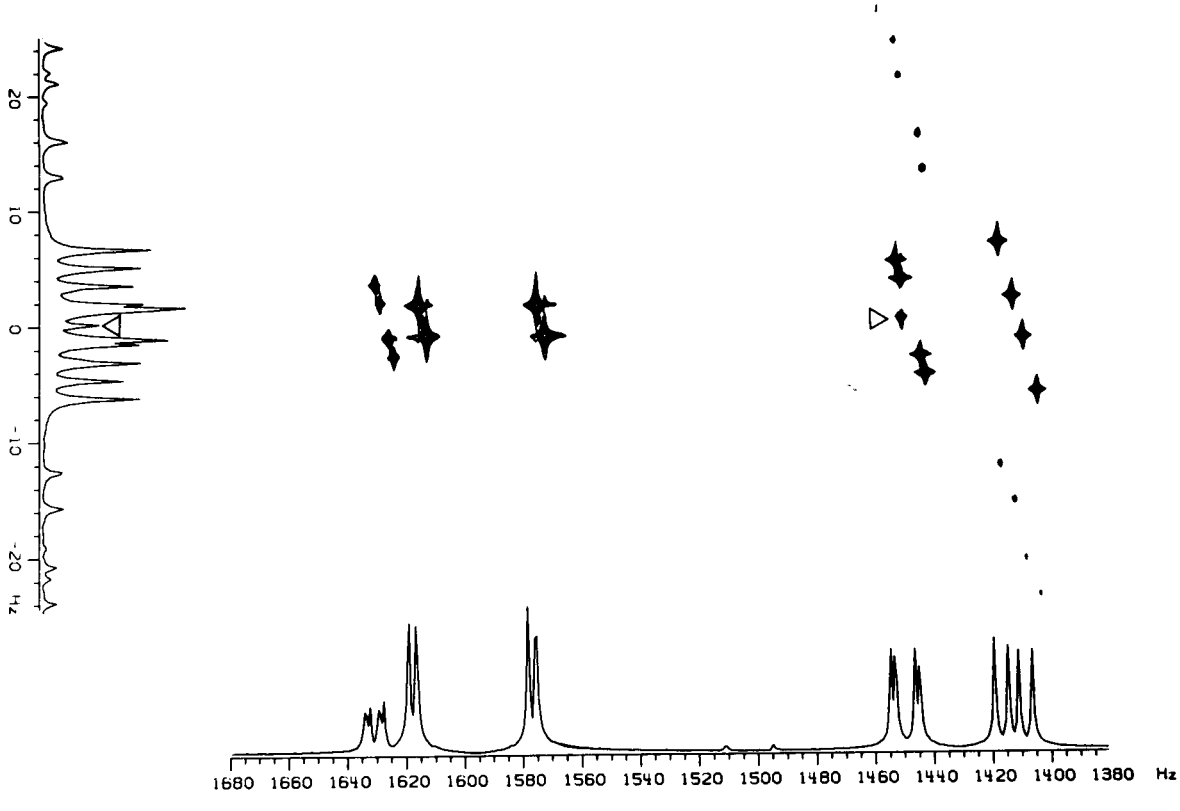


Figure 3. Four level contour plot of the homonuclear 2DJ spectrum of 1,4,9-triazaphenoxathiin (**6**) in deuteriochloroform at 200 MHz. The spectrum was plotted from the $S(F_2, F_1)$ data matrix prior to tilting. To normal spectrum ($F_2$) was obtained from the 90° projection of the data matrix while the J-spectrum was obtained from a 0° projection. Responses designated with open triangles are due to residual protiochloroform.

Table II

Frequencies and Intensities of the X Transitions in the 2DJ Spectrum of an ABX Spin System

| Line pqrs | $F_1$ | $F_2$ (a) | I |
|---|---|---|---|
| 7812 | $\frac{1}{2}(J_{AX} + J_{BX})$ | $\frac{1}{2}(J_{AX} + J_{BX})$ | 1 |
| 4536 | $D_+ + D_-$ | $D_+ + D_-$ | $\sin^2\Sigma \sin^2\Delta$ |
| 4635 | $D_+ - D_-$ | $D_+ - D_-$ | $\cos^2\Sigma \cos^2\Delta$ |
| 4535 | $D_+$ | $D_+ - D_-$ | $-\frac{1}{4}\sin^2\Sigma \sin^2\Delta$ |
| 4636 | $D_+$ | $D_+ + D_-$ | $-\frac{1}{4}\sin^2\Sigma \sin^2\Delta$ |
| 3536 | $D_-$ | $D_+ + D_-$ | $+\frac{1}{4}\sin^2\Sigma \sin^2\Delta$ |
| 4546 | $D_-$ | $D_- - D_+$ | $+\frac{1}{4}\sin^2\Sigma \sin^2\Delta$ |
| 1278 | $-\frac{1}{2}(J_{AX} + J_{BX})$ | $-\frac{1}{2}(J_{AX} + J_{BX})$ | 1 |
| 3645 | $-(D_+ + D_-)$ | $-D_+ - D_-$ | $\sin^2\Sigma \sin^2\Delta$ |
| 3546 | $-(D_+ - D_-)$ | $D_- - D_+$ | $\cos^2\Sigma \cos^2\Delta$ |
| 3545 | $-D_+$ | $D_- - D_+$ | $-\frac{1}{4}\sin^2\Sigma \sin^2\Delta$ |
| 3646 | $-D_+$ | $-D_+ - D_-$ | $-\frac{1}{4}\sin^2\Sigma \sin^2\Delta$ |
| 3635 | $-D_-$ | $-D_+ - D_-$ | $+\frac{1}{4}\sin^2\Sigma \sin^2\Delta$ |
| 4645 | $-D_-$ | $D_+ - D_-$ | $+\frac{1}{4}\sin^2\Sigma \sin^2\Delta$ |
| 3535 | 0 | $D_+ - D_-$ | $\sin^2\Sigma \cos^2\Delta$ |
| 4646 | 0 | $D_- - D_+$ | $\sin^2\Sigma \cos^2\Delta$ |
| 3636 | 0 | $D_+ + D_-$ | $\cos^2\Sigma \sin^2\Delta$ |
| 4545 | 0 | $-D_+ - D_-$ | $\cos^2\Sigma \sin^2\Delta$ |

$\Sigma = \theta_+ + \theta_-$; $\Delta = \theta_+ - \theta_-$; $2D_+ \sin 2\theta_+ = J_{AB}$; $2D_- \sin 2\theta_- = J_{AB}$; $\theta_+$ and $\theta_-$ are small for near first order; $\theta_+ = 90°$; $\theta = 180°$ for non-first order limit. (a) Relative to $\nu_X$.

ly attractive, the complicating influences due to strong coupling counterbalance the benefits of multiplet symmetry and require a careful analysis if the spectrum is to provide useful information.

In the case of strong coupling, already analyzed in several cases [15,17], there is a mixing of the basis functions by the 180° pulse. This mixing leads to linear combinations of the basis functions [10]. As a consequence of the formation of these linear combinations, coherent magnetization associated with the transition $\nu_{pq}$ is converted into a family of magnetization components, e.g., $\nu_{rs}$, $\nu_{tu}$, ..., etc. The corresponding J-spectrum derived from this type of system thus exhibits more "signals" than would by anticipated from the first-order spectrum. These additional resonances in the 2DJ spectrum appear at frequencies of the type $\frac{1}{2}$ ($\nu_{rs} - \nu_{tu}$), etc., with symmetry about $F_1 = 0$ Hz preserved. For a more complete description of this phenomenon, the interested reader is referred to the treatment of Bax [20]. Intensities of responses of this type, as well as the normal responses contained in the 2DJ spectrum, may be computed by the methods described by Kumar [9] or Bodenhausen and co-workers [10], to which the interested reader is referred for a more complete discussion. It is, however, important to note that this development also predicts spectral responses in phase sensitive 2DJ spectra which may have both positive and negative intensities, a result which has been experimentally confirmed both previously [10] and in this work, a facet which must be considered when the signal intensities are computed.

The J-resolved spectrum of **6** in Figures 2A and 2B is clearly more complex in the A and B region from 7.00 to 7.25 ppm than might be anticipated from the one-dimensional spectrum. Frequencies and intensities of the responses in this region of the spectrum were predicted on the basis of the expressions contained in Table I [9,10,21]. The corresponding resonances for the X spin of the ABX spin system were derived from the expressions contained in Table II. Calculated and observed frequencies and intensities for the ABX spin system are gathered in Table III and are illustrated by the slices of the $S(F_1, F_2)$ spectrum labeled A, D and F in Figure 4. Expressions for the AB spin system are presented in Table IV; while the calculated and observed frequencies and intensities at 100 MHz are given in Table V. The corresponding calculated and observed frequencies and intensities for the ABX and AB spin systems at 200 MHz are contained in Tables VI and VII respectively.

Resonances arising by virtue of the strong coupling of the spin systems, mentioned briefly above, are dependent upon the spectrometer frequency [17]. To facilitate the comparison of the 2DJ spectra obtained at 100 and 200 MHz, the resonances due to strong coupling in the ABX and AB spin systems from these spectra are collected in Tables VIII and IX respectively. Given the expressions:

$$\tan 2\theta_+ = J_{AB}/\Delta\nu + \tfrac{1}{2}(J_{AX} - J_{BX}) \qquad (1)$$

$$\tan 2\theta_- = J_{AB}/\Delta\nu - \tfrac{1}{2}(J_{AX} - J_{BX}) \qquad (2)$$

and

$$D_+ = \tfrac{1}{2}\{[\Delta\nu + \tfrac{1}{2}(J_{AX} - J_{BX})]^2 + J_{AB}^2\}^{1/2} \qquad (3)$$

$$D_- = \tfrac{1}{2}\{[\Delta\nu - \tfrac{1}{2}(J_{AX} - J_{BX})]^2 + J_{AB}^2\}^{1/2} \qquad (4)$$

we observe that as the term in $\nu$ Hz is reduced in equations 1 and 2, the denominator approaches zero and so $\theta_+$ and $\theta_-$ become larger. The term $\theta_+$ getting larger at a somewhat slower rate then $\theta_-$. In addition, both $D_-$ and $D_+$ become smaller as $\Delta\theta$ decreases according to equations 3 and 4. The consequences of these trends are shown in Table VIII and may be summarized as follows: as the sum

Table III

Calculated and Observed Frequencies and Intensities for the ABX Spin System of **6** at 100 MHz.

Resonances in the AB Region of the Spectrum

| Trans. Line | | obs. F1 | obs. F2 | calcd. F1 | calcd. F2 | obs. I | calcd. I |
|---|---|---|---|---|---|---|---|
| 1368 | A | -6.39 | 697.1 | -6.4 | 697.0 | 1.000 | 0.864 |
| 2547 | B | -1.82 | 701.7 | -1.8 | 701.6 | 0.899 | 0.803 |
| 1458 | C | -4.93 | 718.8 | -5.0 | 718.6 | 0.793 | 0.803 |
| 2637 | D | -3.29 | 720.4 | -3.2 | 720.4 | 0.906 | 0.864 |
| 1358 | E | 4.45 | 718.8 | 4.4 | 718.6 | 0.571 | 0.386 |
| 2537 | F | 7.56 | 720.4 | 7.6 | 720.4 | 0.594 | 0.386 |
| 2647 | G | -12.61 | 701.4 | -12.6 | 701.6 | -0.286 | -0.241 |
| 1468 | H | -15.71 | 697.1 | -15.8 | 697.0 | -0.279 | -0.241 |
| 6813 | I | 6.38 | 709.9 | 6.4 | 709.8 | 0.971 | 0.864 |
| 4725 | J | 1.80 | 705.3 | 1.8 | 705.2 | 0.961 | 0.803 |
| 5814 | K | 4.98 | 728.6 | 5.0 | 728.6 | 0.838 | 0.803 |
| 3726 | L | 3.36 | 727.0 | 3.2 | 726.8 | 0.870 | 0.864 |
| 5813 | M | -4.48 | 709.9 | -4.4 | 709.8 | 0.601 | 0.386 |
| 3725 | N | -7.57 | 705.3 | -7.6 | 705.2 | 0.591 | 0.386 |
| 4726 | O | 12.40 | 727.0 | 12.6 | 726.8 | -0.244 | -0.241 |
| 6814 | P | 15.71 | 728.6 | 15.8 | 728.6 | -0.279 | -0.241 |

Resonances in the X region of the spectrum

| Trans Line | | obs. F1 | obs. F2 | calcd. F1 | calcd. F2 | obs. I | calcd. I |
|---|---|---|---|---|---|---|---|
| 1278 | A | -3.1 | 811.1 | -3.2 | 811.0 | 0.539 | 1.00 |
| 7812 | B | 3.1 | 817.6 | 3.2 | 817.5 | 0.584 | 1.00 |
| 4536 | C | | | | | | 0.00 |
| 3645 | D | | | | | | 0.00 |
| 4635 | E | -1.4 | 812.8 | -1.4 | 812.9 | 0.474 | 0.83 |
| 3546 | F | 1.4 | 815.8 | 1.4 | 815.7 | 0.591 | 0.83 |
| 4535 | G | | | | | | 0.00 |
| 3545 | H | | | | | | 0.00 |
| 4636 | I | | | | | | 0.00 |
| 3646 | J | | | | | | 0.00 |
| 3536 | K | | | | | | 0.00 |
| 3635 | L | | | | | | 0.00 |
| 4546 | M | | | | | | 0.00 |

| | | | | | | | |
|---|---|---|---|---|---|---|---|
| 4645 | N | | | | | | 0.00 |
| 3535 | O | 0.00 | 812.8 | 0.0 | 812.9 | Seen but not | 0.17 |
| 4646 | P | 0.00 | 815.8 | 0.0 | 815.7 | measurable | 0.17 |
| 3636 | Q | | | | | | 0.00 |
| 4545 | R | | | | | | 0.00 |

$J_{AB}$ = 8.2 Hz; $J_{AX}$ = 1.58 Hz; $J_{BX}$ = 4.8 Hz; $\nu_x$ = 814.25 Hz; $\nu_A$ = 722.82 Hz; $\nu_B$ = 704.38 Hz; $\nu_A - \nu_B$ = 18.44; $D_+$ = 9.36; $D_-$ = 10.84; $\theta_+$ = 13.0°; $\theta_-$ = 11.1°.

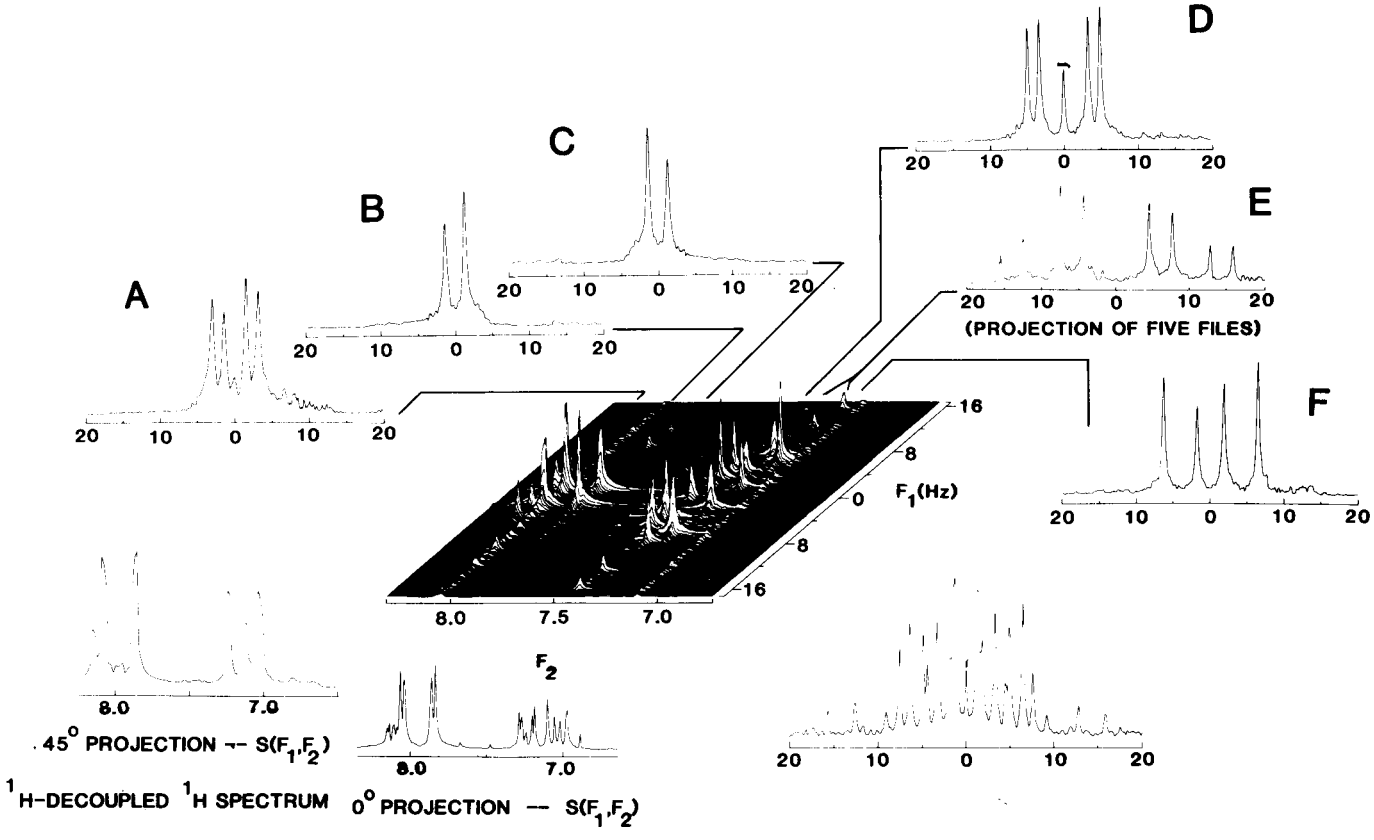


Figure 4. Composite showing a white-washed stack plot of the $S(F_1,F_2)$ matrix at 100 MHz (center) with a proton decoupled proton spectrum obtained by a 45° projection (bottom left), a normal spectrum obtained by a 0° projection (bottom center) and a J-spectrum obtained by a 90° projection (bottom right). Individual slices taken from the $S(F_2,F_1)$ matrix after tilting show the multiplets of the ABX spin system (traces A, D and F) and the AB spin system (taces B and C). The resonances due to strong coupling in the ABX spin system are shown in trace E which is a projection of five contiguous files from the tilted $S(F_2,F_1)$ data matrix.

of the angles approach 90°, the intensity of the "first order" lines in the 2DJ spectrum shifts to those lines due to the strong couplings. As $D_-$ and $D_+$ diminish in value, the lines due to strong coupling also move toward $F_1$ = 0 Hz. Illustration of this consequence as a result of changing spectrometer frequency is dramatically illustrated in Figures 2B and 3. By virtue of the increased spectrometer frequency, the term $\theta_\pm$ decreases in size resulting in the diminution in intensity of the strong coupling signals accompanied by an outward shift (away from $F_1$ = 0 Hz) as shown in Figure 3 relative to Figure 2B. Finally, in the case of the AB spin system, a similar situation develops. As will be noted from the examination of Figure 2A, a set of resonances are visible which are analogous to those of the ABX spin system (these resonances do not appear in Figure 2B at the contour levels employed). As will be noted

Table IV

Frequencies and Intensities in the 2DJ Spectrum of an AB Spin System

| Line pqrs | $F_1$ | $F_2$ (a) | I |
|---|---|---|---|
| 1334 | $-C - \frac{1}{2}J$ | $-C - \frac{1}{2}J$ | $-\sin 2\theta\,(1 - \sin 2\theta)$ |
| 3413 | $+C + \frac{1}{2}J$ | $+C + \frac{1}{2}J$ | $-\sin 2\theta\,(1 - \sin 2\theta)$ |
| 1324 | $-\frac{1}{2}J$ | $+C - \frac{1}{2}J$ | $\cos^2 2\theta$ |
| 2413 | $+\frac{1}{2}J$ | $+C + \frac{1}{2}J$ | $\cos^2 2\theta$ |
| 1224 | $+C - \frac{1}{2}J$ | $+C - \frac{1}{2}J$ | $\sin 2\theta\,(1 + \sin 2\theta)$ |
| 2412 | $-C + \frac{1}{2}J$ | $-C + \frac{1}{2}J$ | $\sin 2\theta\,(1 + \sin 2\theta)$ |
| 1234 | $-\frac{1}{2}J$ | $-C - \frac{1}{2}J$ | $\cos^2 2\theta$ |
| 3412 | $+\frac{1}{2}J$ | $-C + \frac{1}{2}J$ | $\cos^2 2\theta$ |

$2C = [(\nu_A - \nu_B)^2 + J^2]^{1/2}$; $\tan 2\theta = J/(\nu_A - \nu_B)$; (a) measured relative to $(\nu_A + \nu_B)/2$

from Table IX, the change in spectrometer frequency from 100 to 200 MHz decreases the intensities to the point that they were not readily detectable in the 2DJ spectrum of **6** with the available signal-to-noise ratio.

Similar, although considerably less pronounced behavior is observed in the case of the X spin as well. As will be noted from Table III, a considerable number of resonance lines are predicted for the X-spin although they are of negligible intensity when the term $\Delta\nu >> (J_{AX} - J_{BX})$. These resonances begin to take on measureable intensity when $\Delta\nu \geq (J_{AX} - J_{BX})$ and both $\Delta$ and $\Sigma$ gain gain significant intensity. The net result of these occurrences is the conversion of the simple four line 2DJ multiplet into a pattern of as many as eighteen weaker resonances which may be difficult to resolve in spectra where limited digital resolution is available. To illustrate this type of behavior, we have calculated the frequencies and intensities of the resonances for the ABX spin system at spectrometer frequencies of 60 and 30 MHz which are shown in Tables X and XI respectively. The degree of complication produced under these conditions is analogous to what might be expected for more strongly coupled spin systems than those of the model system at hand when examined at 100 MHz. The improvement in the X spin obtained on going from 30 to 100 MHz is also comparable to what would be obtained in going from 100 to 300 MHz for the AB region of the ABX spin system.

From this example, it is clear that resorting to a 2DJ spectroscopy will not necessarily solve spectral interpretation problems if undertaken blindly. On the other hand, 2DJ spectra can still be highly useful in the analysis of complicated spin systems, the presence of resonances due to strong coupling even aiding in the analysis in some cases. Every resonance, whether first or higher order, in the 2DJ spectrum of 1,4,9-triazaphenoxathiin (**6**) has been identified and assigned.

## EXPERIMENTAL

Melting points were obtained on a Thomas-Hoover melting point apparatus in open capillaries and are reported uncorrected. Infrared spectra were taken as potassium bromide pellets on a Perkin-Elmer Model 283 spectrophotometer. Mass spectra were obtained using a Hewlett-Packard Model 5930 GC/MS system equipped with Model 5933A data system *via* direct probe insertion with a source temperature of 250° and an ionizing energy of 70 eV. Microanalysis was performed by Atlantic Microlabs, Atlanta, GA. The nmr spectrometers employed in this work consisted of a Varian XL-100-15 spectrometer equipped with a Nicolet

Table V

Calculated and Observed Frequencies and Intensities for the AB Spin System of **6** at 100 MHz

| Trans Line | | obs. F1 | obs. F2 | calcd. F1 | calcd. F2 | obs. I | calcd. I |
|---|---|---|---|---|---|---|---|
| 1334 | A | 11.73 | 808.5 | 11.76 | 808.5 | -0.120 | -0.111 |
| 3413 | B | 1.33 | 808.5 | 1.33 | 808.5 | 1.006 | 0.984 |
| 1324 | C | 9.19 | 805.8 | 9.10 | 805.9 | 0.126 | 0.143 |
| 2413 | D | -1.33 | 805.8 | -1.33 | 805.9 | 0.126 | 0.143 |
| 1224 | E | 1.33 | 787.7 | 1.33 | 787.7 | 0.995 | 0.984 |
| 2412 | F | -9.14 | 787.7 | -9.10 | 787.7 | 0.150 | 0.143 |
| 1234 | G | -1.33 | 785.0 | -1.33 | 785.0 | 0.985 | 0.984 |
| 3412 | H | -11.71 | 785.0 | -11.76 | 785.0 | -0.122 | -0.111 |

$J = 2.65$; $\nu_A = 807.13$; $\nu_B = 786.44$; $\nu_A - \nu_B = 20.69$; $(\nu_A + \nu_B)/2 = 796.78$; $C = 10.43$; $\theta = 3.65°$.

Table VI

Calculated and Observed Frequencies and Intensities for the ABX Spin System of **6** at 200 MHz

Resonances in the AB region of the spectrum

| Trans. Line | | obs. F1 | obs. F2 | calcd. F1 | calcd. F2 | obs. I | calcd. I |
|---|---|---|---|---|---|---|---|
| 1368 | A | -6.36 | 1401.8 | -6.48 | 1401.8 | 0.896 | 0.962 |
| 2547 | B | -1.77 | 1406.6 | -1.72 | 1406.6 | 0.892 | 0.944 |
| 1458 | C | -4.77 | 1441.4 | -4.92 | 1441.2 | 0.749 | 0.944 |
| 2637 | D | -3.28 | 1443.0 | -3.28 | 1442.8 | 0.908 | 0.962 |
| 1358 | E | 13.0 | 1441.4 | 13.19 | 1441.2 | 0.211 | 0.214 |
| 2537 | F | 16.3 | 1443.0 | 16.39 | 1442.8 | 0.249 | 0.214 |
| 2647 | G | -21.3 | 1406.6 | -21.39 | 1406.6 | -0.143 | -0.170 |
| 1468 | H | -24.4 | 1401.8 | -24.59 | 1401.8 | -0.145 | -0.170 |
| 6813 | I | 6.34 | 1414.6 | 6.48 | 1414.8 | 1.000 | 0.962 |
| 4725 | J | 1.87 | 1410.2 | 1.72 | 1410.0 | 0.931 | 0.944 |
| 5814 | K | 4.97 | 1451.0 | 4.92 | 1451.0 | 0.905 | 0.944 |
| 3726 | L | 3.24 | 1449.4 | 3.28 | 1449.4 | 0.843 | 0.962 |
| 5813 | M | -13.0 | 1414.6 | -13.19 | 1414.8 | 0.199 | 0.214 |
| 3725 | N | -16.3 | 1410.2 | -16.39 | 1410.0 | 0.207 | 0.214 |
| 4726 | O | 21.3 | 1449.4 | 21.39 | 1449.4 | -0.167 | -0.170 |
| 6814 | P | 24.4 | 1451.0 | 24.59 | 1451.0 | -0.202 | -0.170 |

Resonances in the X Region of the Spectrum.

| Trans Line | | obs. F1 | obs. F2 | calcd. F1 | calcd. F2 | obs. I | calcd. I |
|---|---|---|---|---|---|---|---|
| 7812 | A | 3.16 | 1631.7 | 3.20 | 1631.7 | 0.381 | 1.000 |
| 1278 | B | −3.06 | 1625.5 | −3.20 | 1625.3 | 0.475 | 1.000 |
| 4536 | C | | | | | | |
| 3645 | D | | | | | | |
| 4635 | E | −1.38 | 1630.2 | -1.56 | 1630.0 | 0.422 | 0.953 |
| 3546 | F | 1.36 | 1627.1 | 1.56 | 1626.9 | 0.406 | 0.953 |
| 4535 | G | | | | | | |
| 3545 | H | | | | | | |
| 3636 | I | | | | | | |
| 3646 | J | | | | | | |
| 3536 | K | | | | | | |
| 3635 | L | | | | | | |

| | | | | |
|---|---|---|---|---|
| 4546 | M | | | |
| 4645 | N | | | |
| 3535 | O | 0.00 | 1630.0 | 0.047 |
| 4646 | P | 0.00 | 1626.9 | 0.047 |
| 3636 | Q | | | |
| 4545 | R | | | |

$J_{AB}$ = 8.2 Hz; $J_{AX}$ = 1.58 Hz; $J_{BX}$ = 4.8 Hz; $\nu_X$ = 1628.50 Hz; $\nu_A$ = 1445.64 Hz; $\nu_B$ = 1408.76 Hz; $\nu_A - \nu_B$ = 36.88 Hz; $(\nu_A + \nu_B)/2$ = 1427.20 Hz; $D_+$ = 18.11; $D_-$ = 19.67; $\theta_+$ = 6.02°; $\theta_-$ = 6.54°.

Table VII.

Calculated and Observed Frequencies and Intensities for an AB Spin System of **6** at 200 MHz

| Trans Line | | obs. F1 | obs. F2 | calcd. F1 | calcd. F2 | obs. I | calcd. I |
|---|---|---|---|---|---|---|---|
| 1334 | A | 21.89 | 1618.57 | 22.02 | 1618.76 | -0.070 | -0.062 |
| 3413 | B | 1.36 | 1618.57 | 1.38 | 1618.76 | 0.901 | 0.996 |
| 1324 | C | 19.30 | 1616.11 | 19.27 | 1616.01 | 0.047 | 0.062 |
| 2413 | D | -1.32 | 1616.11 | -1.38 | 1616.01 | 0.871 | 0.996 |
| 1224 | E | 1.36 | 1577.49 | 1.38 | 1577.48 | 1.000 | 0.996 |
| 2412 | F | -19.26 | 1577.49 | -19.27 | 1577.48 | 0.040 | 0.062 |
| 1234 | G | -1.32 | 1574.78 | -1.38 | 1574.73 | 0.844 | 0.996 |
| 3412 | H | -21.85 | 1574.78 | -22.02 | 1574.73 | -0.070 | -0.062 |

J = 2.65 Hz; $\nu_A$ = 1617.33; $\nu_B$ = 1576.15 Hz; $\nu_A - \nu_B$ = 41.18; $(\nu_A + \nu_B)/2$ = 1596.74 Hz; C = 20.64 Hz; $\theta$ = 1.91°.

Table VIII

Resonances Due to Strong Coupling in the ABX Spin System of **6** at 100 and 200 MHz
Resonances in the AB Region of the Spectrum

| | 100 MHz | | | 200 MHz | | |
|---|---|---|---|---|---|---|
| Trans. Line | obs. F1 | obs. F2 | obs. I | obs. F1 | obs. F2 | obs. I |
| 6814 | 15.7 | 728.6 | -0.279 | 24.4 | 1451.0 | -0.202 |
| 4726 | 12.4 | 727.0 | -0.244 | 21.3 | 1449.4 | -0.167 |
| 2537 | 7.6 | 720.4 | 0.574 | 16.3 | 1443.0 | 0.249 |
| 1358 | 4.5 | 718.8 | 0.571 | 13.0 | 1441.4 | 0.211 |
| 5813 | -4.5 | 709.9 | 0.601 | -13.0 | 1414.6 | 0.199 |
| 3725 | -7.6 | 705.3 | 0.591 | -16.3 | 1410.2 | 0.207 |
| 2647 | -12.6 | 701.7 | -0.286 | -21.3 | 1406.6 | -0.143 |
| 1468 | -15.7 | 697.1 | -0.279 | -24.4 | 1401.8 | -0.145 |

Resonances in the X region of the spectrum

| Trans. Line | obs. F1 | obs. F2 | obs. I | calcd. F1 | calcd. F2 | calcd. I |
|---|---|---|---|---|---|---|
| 3535 | 0.0 | 812.8 | 0.17 | 0.0 | 1630.0 | 0.047 |
| 4646 | 0.0 | 815.8 | 0.17 | 0.0 | 1626.9 | 0.047 |

Table IX

Resonances Due to Strong Coupling in the AB Spin System

| | | 100 MHz | | | 200 MHz (b) | | |
|---|---|---|---|---|---|---|---|
| Trans. Line | | obs. F1 | obs. F2 | obs. I | calcd. F1 | obs. F2 | calcd. I |
| 1334 | A | 11.7 | 808.5 | -0.12 (a) | 22.02 | 1618.57 | -0.062 |
| 1324 | C | 9.2 | 805.8 | 0.13 | 19.27 | 1616.11 | 0.062 |
| 2412 | F | -9.1 | 787.7 | 0.15 | -19.27 | 1577.49 | 0.062 |
| 3412 | H | -11.7 | 785.0 | -0.12 (a) | -22.02 | 1574.78 | -0.062 |

(a) Intensities of these resonances were shown to be negative from phase sensitive plots [9,10]. (b) Resonances due to strong coupling were not visible in the 200 MHz 2DJ spectrum with the signal to noise level available (see Figure 3).

1180 computer interfaced through a 293A' pulse programmer and a NIC-200 spectrometer equipped with a Nicolet 1280 computer also interfaced through a Model 293A' pulse programmer. Specific instruments parameters employed in the conduct of the 2DJ experiments are summarized below.

Synthesis of 1,4,9-Triazaphenoxathiin (**6**).

The 2,3-dichloropyrazine (**2**) required for the synthesis of 1,4,9-triazaphenoxathiin (**6**) was obtained from the chlorination of 2-chloropyrazine (**1**) with sulfuryl chloride in *N,N*-dimethylformamide (DMF) according to the procedure of Okafor [18], the product fractionally distilled prior to use. Thus, to 1.634 g (0.013 mmoles) of 3-hydroxypyridine-2(1*H*)-thione in 30 ml of dry, freshly distilled DMF was added 0.70 g (0.029 moles) of sodium hydride as 99% dry powder under an inert argon atmosphere. The resultant suspension was stirred at room temperature for 6 hrs, after which was added 1.49 g (0.010 moles) in an additional 10 ml of dry, distilled DMF. The resultant solution darkened almost immediately, was stirred at room temperature for 1 hour and was then brought to reflux temperature for 1 hour. Upon cooling, the dark colored solution was poured into 300 ml of ice cold distilled water, the resultant aqueous solution then extracted with 4 × 200 ml of ethyl acetate. The ethyl acetate extracts were combined, back extracted with 4 × 200 ml of distilled water and then dried over anhydrous sodium sulfate. The ethyl acetate solution was then evaporated *in vacuo* to give an oily residue which was chromatographed over a silica column gradient eluted with a solvent mixture varied from pure heptane to heptane:ethyl acetate (6:1) to give **6** as nearly colorless crystals, 1.29 g (64% yield), mp 160-161°; ms: m/e (% relative intensity) 203 (100) (molecular ion, $M^+$), M + 1, 204 (12.3), M + 2, 205 (6.3), $M^+$ − HCN, 176 (6.7), $M^+$ − CO, 175 (5.5), $M^+$ − S, 171 (1.3), $M^+$ − CS, 159 (20.8), 148 (4.4), 121 (4.1).

*Anal.* Calcd. for $C_9H_5N_3OS$: C, 53.20; H, 2.46; N, 20.69. Found: C, 53.43; H, 2.54; N, 20.76.

Acquisition and Processing of the 2DJ Data.

A reference spectrum of **6** was taken at 100 MHz with a total spectral width of 200 Hz (quadrature data) digitized with 8K data points (see

Table X

Calculated Frequencies and Intensities for the ABX Spin System of **6** at 60 MHz

Resonances in the AB Region of the Spectrum

| Line | $F_1$ | $F_2$ | I |
|---|---|---|---|
| 1368 | -5.06 | -11.97 | 0.70 |
| 2547 | -3.15 | -10.06 | 0.59 |
| 1458 | -6.35 | 0.57 | 0.59 |
| 2637 | -1.86 | 5.06 | 0.70 |
| 1358 | 1.22 | 0.57 | 0.52 |
| 2537 | 4.42 | 5.06 | 0.52 |
| 2647 | -9.42 | -10.06 | 0.44 |
| 1468 | -12.62 | -11.97 | 0.44 |
| 6813 | 5.06 | -1.86 | 0.70 |
| 4725 | 3.15 | -3.77 | 0.59 |
| 5814 | 6.35 | 13.26 | 0.59 |
| 3726 | 1.86 | 8.77 | 0.70 |
| 5813 | -1.22 | -1.86 | 0.52 |
| 3725 | -4.42 | -3.77 | 0.52 |
| 4726 | 9.42 | 8.77 | 0.44 |
| 6814 | 12.62 | 13.26 | 0.44 |

Resonances in the X Region of the Spectrum

| Line | $F_1$ | $F_2$ | I |
|---|---|---|---|
| 7812 | 3.2 | 3.2 | 1.00 |
| 4536 | 13.83 | 13.83 | 0.00 |
| 4635 | 1.29 | 1.29 | 0.64 |
| 4535 | 7.56 | 1.29 | -0.03 |
| 4636 | 7.56 | 13.83 | -0.03 |
| 3536 | 6.27 | 13.83 | 0.03 |
| 4546 | 6.27 | -1.29 | 0.03 |
| 1278 | -3.2 | -3.20 | 1.00 |
| 3645 | -13.83 | -13.83 | 0.00 |
| 3546 | -1.29 | -1.29 | 0.64 |
| 3545 | -7.56 | -1.29 | -0.03 |
| 3646 | -7.56 | -13.83 | -0.03 |
| 3635 | -6.27 | -13.83 | 0.03 |
| 4645 | -6.27 | 1.29 | 0.03 |
| 3535 | 0.00 | 1.29 | 0.36 |
| 4646 | 0.00 | -1.29 | 0.36 |
| 3636 | 0.00 | 13.83 | 0.00 |
| 4545 | 0.00 | -13.83 | 0.00 |

$J_{AB}$ = 8.2 Hz; $J_{AX}$ = 1.6 Hz; $J_{BX}$ = 4.8 Hz; $\nu_X$ = 488.6 Hz; $\nu_A$ = 433.7 Hz; $\nu_B$ = 422.6 Hz; $\nu_A - \nu_B$ = 11 Hz; $(\nu_A + \nu_B)/2$ = 428.15 Hz; $D_+$ = 7.56; $D_-$ = 6.27; $\theta_+$ = 16.42; $\theta_-$ = 20.40.

Figure 1). Based on the spectrum, the 2DJ spectra at 100 and 200 MHz were taken with spectral widths of 200 and 400 Hz (quadrature) digitized with 1K and 2K data points respectively. Delays in the evolution period were selected to give a total spectral width in $F_1$ = ± 25 Hz, the spectrum digitized by 256 incrementations of $t_1$ in this dimension to give a digital resolution of 0.19 Hz in $F_1$. The pulse sequence employed was the standard 90° − $\tau$ − 180° − $\tau$ − aquire sequence supplied with the Nicolet NTCFT/NMC operating software packages. Pulse widths on the two spectrometers utilized were calibrated using a standard dioxane in benzene sample to minimize artifacts which may arise due to an improperly calibrated 180° refocusing pulse [22,23]. Measured 90° pulses were thus 22 μseconds and 7.9 μseconds at 100 and 200 MHz respectively.

The 2DJ data acquired in the experiments were processed in both cases by first transforming the first block of the $S(t_1,t_2)$ data set after exponential multiplication of the FID with a 0.1 Hz time constant. This spectrum was then phased and scaled after which the remaining 255 blocks of data were Fourier transformed with respect to $t_2$ using established phasing and scaling parameters. After transposition to provide the $S(F_2, t_1)$ data array, the largest interferogram was selected, subjected to exponential multiplication with a 0.1 Hz time constant and Fourier transformed. The resultant spectrum was magnitude calculated

Table XI

Calculated Frequencies and Intensities for the ABX Spin System of **6** at 30 MHz

Resonances in the AB Region of the Spectrum

| Line | $F_1$ | $F_2$ | I |
|---|---|---|---|
| 1368 | -5.26 | -7.42 | 0.37 |
| 2547 | -0.89 | -5.12 | 0.23 |
| 1458 | -4.09 | 1.58 | 0.23 |
| 2637 | -0.01 | 5.68 | 0.37 |
| 1358 | 1.33 | 1.58 | 0.57 |
| 2537 | 4.53 | 5.68 | 0.57 |
| 2647 | -5.43 | -5.12 | 0.35 |
| 1468 | -8.63 | -7.42 | 0.35 |
| 6813 | 5.26 | -2.40 | 0.37 |
| 4725 | 0.89 | -4.70 | 0.23 |
| 5814 | 4.09 | 8.42 | 0.23 |
| 3726 | 0.01 | 4.34 | 0.37 |
| 5813 | -1.33 | -2.40 | 0.57 |
| 3725 | -4.53 | -4.70 | 0.57 |
| 4726 | 5.43 | 4.34 | 0.35 |
| 6814 | 8.63 | 8.42 | 0.35 |

Resonances in the X Region of the Spectrum

| Line | $F_1$ | $F_2$ | I |
|---|---|---|---|
| 7812 | 3.20 | 3.20 | 1.00 |
| 4536 | 9.97 | 9.97 | 0.01 |
| 4635 | 0.89 | 0.89 | 0.30 |
| 4535 | 5.43 | 0.89 | -0.06 |
| 4636 | 5.43 | 9.97 | -0.06 |
| 3536 | 4.54 | 9.97 | 0.06 |
| 4546 | 4.54 | -0.89 | 0.06 |
| 1278 | 3.20 | -3.20 | 1.00 |
| 3645 | 9.97 | -9.97 | 0.01 |
| 3546 | 0.89 | -0.89 | 0.30 |
| 3545 | 5.43 | -0.89 | -0.06 |
| 3646 | 5.43 | -9.97 | -0.06 |

| | | | |
|---|---|---|---|
| 3635 | 4.54 | -9.97 | 0.06 |
| 4645 | 4.54 | -0.89 | 0.06 |
| 3535 | 0.00 | 0.89 | 0.69 |
| 4646 | 0.00 | -0.89 | 0.69 |
| 3636 | 0.00 | 9.97 | 0.01 |
| 4545 | 0.00 | -9.97 | 0.01 |

$J_{AB}$ = 8.2 Hz; $J_{AX}$ = 1.6 Hz; $J_{BX}$ = 4.8 Hz; $\nu_X$ = 244.3 Hz; $\nu_A$ = 216.8 Hz; $\nu_B$ = 211.32 Hz; $\nu_A - \nu_B$ = 5.52 Hz; $D_+$ = 5.43; $D_-$ = 4.54; $\theta_+$ = 24.5°; $\theta_-$ = 32.22°.

to establish scaling parameters for the second Fourier transform with respect to $t_1$. The spectrum shown in Figure 2A is a white-washed stack plot of the $S(F_1,F_2)$ data matrix prior to tilting [14]. The four level contour plots shown in Figures 2B and 3 were obtained from the $S(F_2,F_1)$ data matrix prior to retransposition. Projections shown in Figure 4 (with the exception of trace E) were prepared directly from the $S(F_2,F_1)$ data matrix. Slices A-D and F were obtained by tilting the $S(F_1,F_2)$ data matrix according to the method of Hall and Sukumar (14) and then plotting the appropriate single files of the $S(F_2, F_1)$ data matrix after transposition. Trace E (Figure 4) is a projection of five contiguous files of the $S(F_2,F_1)$ matrix after tilting and shows the peaks in the AB region of the ABX spin system which are due to strong coupling.

Acknowledgement.

Several of the authors, G. E. M., M. R. W., III, and A. L. T., Jr., acknowledge the generous support of the Robert A. Welch Foundation in the form of Grants Nos. E-792, E-183 and Y-484, which provided a predoctoral fellowship for R. T. G., Jr. and a postdoctoral followship for J J. F. One of the authors, G. E. M., acknowledges the Merck, Sharp and Dohme University Grants program which supported, in part, the synthesis of the title compound. In addition, two of the authors, G. E. M. and K. S., also acknowledge the North Atlantic Treaty Organization which supported the visit of K. S. to Houston through Grant No. 019.81. The authors also wish to acknowledge the National Science Foundation, Grant No. CHE-7506162, for the XL-100 spectrometer system at Houston used for a portion of this work and the National Institutes of Health through Biomedical Research Support Grant No. 2SO7RR7147-07. We would finally like to express our very sincere appreciation of Mrs. Cathy Meier for her perserverence in the preparation of the numerous tables contained in this work.

## REFERENCES AND NOTES

[1] This paper also represents Part 6 in the series "Novel Heterocyclic Systems."

[2] To whom inquiries should be addressed.

[3] On leave at the Department of Chemistry, University of South Florida, Tampa, Florida 33620 during the period when this work was performed.

[4] J. Jeener, abstract of a paper presented at the Ampere International Summer School, Basko Polje, Yugoslavia.

[5] L. Muller, A. Kumar and R. R. Ernst, *J. Chem. Phys.*, **63**, 5490 (1975).

[6] W. P. Aue, E. Bartholdi and R. R. Ernst, *ibid.*, **64**, 2229 (1976).

[7] K. Nagayama, A. Kumar, K. Wuthrich and R. R. Ernst, *J. Magn. Reson.*, **40**, 321 (1980).

[8] W. P. Aue, J. Karhan and R. R. Ernst, *J. Chem. Phys.*, **64**, 4226 (1976).

[9] A. Kumar, *J. Magn. Reson.*, **30**, 227 (1978).

[10] G. Bodenhausen, R. Freeman, G. A. Morris and D. L. Turner, *ibid.*, **31**, 75 (1978).

[11] A. D. Bain, *ibid.*, **39**, 335 (1980).

[12] K. Nagayama, P. Bachman, K. Wuthrich and R. R. Ernst, *ibid.*, **31**, 133 (1978).

[13] S. Brownstein, *ibid.*, **42**, 150 (1981).

[14] L. D. Hall and S. Sukumar, *ibid.*, **38**, 555 (1980).

[15] G. Wider, R. Baumann, K. Nagayama, R. R. Ernst and K. Wuthrich, *ibid.*, **42**, 73 (1981).

[16] P. H. Bolton, *ibid.*, **45**, 239 (1981).

[17] S. Puig-Torres, R. T. Gampe, Jr., G. E. Martin, M. R. Willcott, III and K. Smith, *J. Heterocyclic Chem.*, **20**, 253 (1983).

[18] C. O. Okafor, *ibid.*, **18**, 405 (1981).

[19] C. H. Womack, L. M. Martin, G. E. Martin and K. Smith, *ibid.*, **19**, 1447 (1982).

[20] A. Bax, "Two-Dimensional Nuclear Magnetic Resonance in Liquids", Delft University Press, Delft, Holland obtained through Kluwer-Boston, Inc., Hingham, MA, 1982, pp 116-118.

[21] We have reproduced in Tables I, II and V the expressions for the calculation of the frequencies and intensities of the resonances in the AB and X spin of the ABX system and the AB system respectively. Although these have been previously published (*cf.* refs [9] and [10]), an error was encountered in our initial attempts to utilize the expressions contained in ref [10] for the ABX spin system, thus prompting us to reproduce the expressions in their correct form in this work.

[22] G. Bodenhausen, R. Freeman, R. Niedermeyer and D. L. Turner, *J. Magn. Reson.*, **26**, 133 (1977).

[23] G. Bodenhausen, R. Freeman and D. L. Turner, *ibid.*, **27**, 511 (1977).